Total attenuation coefficients and scattering phase functions of tissues and phantom materials at 633 nm

Stephen T. Flock, Brian C. Wilson,[a] and Michael S. Patterson
Departments of Physics, Hamilton Regional Cancer Centre and McMaster University, Hamilton, Ontario, Canada L8V 1C3

(Received 10 November 1986; accepted for publication 22 June 1987)

Measurements have been made of the total attenuation coefficient Σ_t and the scattering phase function, $S(\theta)$, of 632.8 nm of light for a number of animal model tissues, blood, and inert scattering and absorbing media. Polystyrene microspheres of known size and refractive index, for which Σ_t and $S(\theta)$ can be calculated by Mie theory, were used to test the experimental methods. The purpose of the study was to define typical ranges for these optical properties of tissues, as a contribution to the development of experimental and theoretical methods of light dosimetry in tissue, particularly related to photodynamic therapy of solid tumors. The results demonstrate that, for the representative tissues studied, the total attenuation coefficients are of the order of 10–100 mm^{-1}, and that scattering is highly forward peaked, with average cosine of scatter in the range 0.6–0.97.

I. INTRODUCTION

The rapid development of medical and surgical applications of lasers in the past few years has generated interest in measuring the optical properties of tissues and in developing models of light propagation in tissues. In particular, the development of photodynamic therapy (PDT) has necessitated studies of the optical properties of tissues at wavelengths around 630 nm, this being the wavelength at which the photosensitizer commonly used in PDT, namely hematoporphyrin derivative, is normally activated. The physical aspects of PDT have been reviewed by Wilson and Patterson,[1] including a survey of the published data on tissue optical properties at 630 nm, and current models of light propagation.

The attenuation of visible light in tissue can be considered as due essentially to absorption and elastic scattering. The terms used in this paper to describe these processes are as follows: The coefficients Σ_a and Σ_s, represent the probabilities per unit path length in tissue that a photon will be absorbed or scattered, respectively. Σ_s is related to the differential scattering coefficient $\Sigma_s(\Omega \rightarrow \Omega')$ representing the probability per unit path length per unit solid angle of scatter from solid angle Ω to Ω', so that

$$\Sigma_s = \int_{4\pi} \Sigma_s(\Omega \rightarrow \Omega')\, d\Omega'. \tag{1}$$

The total attenuation coefficient Σ_t is the sum of the absorption and scattering coefficients; its inverse, $1/\Sigma_t$, is the mean free path between photon interactions. The scattering phase function, $S(\theta)$, describes the angular dependence of the scattering, where θ is the angle between the incident beam and the scattered photon, in the scattering plane. $S(\theta)$ is given by

$$S(\theta) = \left(\frac{2\pi}{\Sigma_s}\right) \frac{d\Sigma_s(\Omega \rightarrow \Omega')}{d\Omega'}, \tag{2}$$

where the integral of $S(\theta)$ over 4π sr is unity. This assumes azimuthal symmetry in the scattering process.

In some models of light propagation,[2] a useful simplifying parameter is the mean cosine of scatter,

$$\bar{\mu} = \int_{-1}^{1} S(\theta) \cos\theta d(\cos\theta). \tag{3}$$

Thus, $\bar{\mu} = 0$ represents isotropic scattering, while $0 < \bar{\mu} < 1$ represents forward scattering

Apart from skin, most of the published measurements for tissue optical properties in the visible range have been for the effective attenuation coefficient, Σ_{eff} (see Ref. 1). Studies have been done in animal[3–11] and a few human[12–22] tissues, mainly on *postmortem* specimens. *In vivo* data are sparse.[3,8,10,21,22] For a homogeneous, semi-infinite slab of tissue irradiated by a plane collimated light beam, the space irradiance decreases with depth x from the irradiated surface as $\exp(-\Sigma_{eff}\, x)$. This exponential behavior does not hold near the surface. Although Σ_{eff} is a useful parameter for comparing the general light transmittance characteristics of different tissues and their wavelength dependence,[5,10,11] it is a complex combination of the fundamental coefficients Σ_a, Σ_s, and $S(\theta)$, and, furthermore, measurement of Σ_{eff} may depend on the irradiation and tissue geometries.

There are very few measurements of the separate absorption and scattering parameters, even *in vitro*. To date all the data have been obtained by "indirect" experiments, in which the fundamental coefficients are *derived* from measurements of some macroscopic tissue property such as diffuse transmittance or reflectance,[4,11,14–16,23,24] or a combination of Σ_{eff} and the pattern of radiance at depth.[6,9] The derivation necessarily requires use of some model of light propagation, such as the two-flux method of Kubelka and Munk,[25,26] numerical solution of the transport equation such as used by van de Hulst,[27] Monte Carlo computer calculations,[7,28] or diffusion theory.[3,5,6,9,17,19,29] With the possible exception of Monte Carlo methods, such models generally require simplifying assumptions, or place restrictions on the range of parameter values of geometries for which solutions may be obtained.

 0094-2405/87/050835-07$01.20

The alternative, which avoids model-dependent limitations, is "direct" determination of the optical coefficients. In this, tissue samples are used which are thin enough that multiple scattering may be ignored. To our knowledge, no such experiments have been reported in the visible wavelength range for tissues other than skin.[30] In the present study we report measurements of Σ_t and $S(\theta)$ at 633 nm for four normal animal tissues and one animal solid tumor, as well as for blood and for inert media which have been used in PDT as light scattering or absorption materials.[6,9,21,31] The primary objective was to ascertain the range of values of Σ_t and $S(\theta)$, which typify lightly pigmented soft tissues at this wavelength, rather than to provide an exhaustive or comprehensive survey of these parameters for animal and human tissue. It should be noted that to obtain a complete set of direct data requires that either Σ_a or Σ_s also be measured. However, as discussed elsewhere,[32] there are technical difficulties in this, which have not yet been solved completely, because of the high attenuation and high albedo of tissues.

II. MATERIALS AND METHODS

A. Total attenuation coefficient

The total attenuation coefficient Σ_t was measured using the narrow-beam experiment shown in Fig. 1. The sample, placed between glass microscope cover slips (for solid tissues) or in cuvettes (for suspensions) was irradiated by the 632.8-nm beam from a 5-mW HeNe laser. A 7.6-cm-diam integrating sphere with a radiometer at a 90° port was used to detect the transmitted light beam, scatter being rejected by a 1-mm pinhole placed immediately in front of the integrating sphere entrance port. The half-angle subtended by this aperture from the sample was 0.17°. Use of the integrating sphere plus radiometer rather than the radiometer alone was simply for convenience, since this system has been developed for future direct measurements of Σ_a and Σ_s. The face of the radiometer photodiode was set 2 cm back from the surface of the sphere so that only diffuse light was detected. The detected flux $I(t)$ for sample thickness t was first measured for the tissue or phantom material. This was then immediately repeated with water in the same cell in order to measure the incident light flux, $I_0(t)$. This measurement compensated for losses due to specular reflections at the air–cell and cell–tissue interfaces, since the refractive indices of water and tissue are similar. The laser output was checked between readings to correct for slight variations in the incident light intensity. Σ_t was then calculated from

$$\Sigma_t = (1/t)\ln(I_0/I). \quad (4)$$

The fresh animal tissues were first ground to facilitate preparation of thin tissue samples. In order that the experiments for a given tissue could be extended over several days, the bulk ground tissues were frozen. For each experiment, a sample was thawed, placed on a cover slip, and a second cover slip carefully placed on top. The sample thickness was then determined using a micrometer. For each thickness, several samples were prepared and measured, always from the same tissue batch. Preparation and handling of tissue samples were as consistent between experiments as possible.

For measurements of blood, a fresh human sample was drawn, heparinized, and diluted in 1% phosphate buffered saline. Light microscopy was used to check that no significant red blood cell lysis had occurred. The sample was then placed in the optical cuvette, and measurements made as for tissue. The cuvette was also used for the scattering phantom medium, which comprised different aqueous concentrations of the fat emulsion Nutralipid™ (Pharmacia Inc., Quebec).

As a rigorous check on the measurement technique, Σ_t was determined in the same way for an aqueous suspension of polystyrene microspheres (Seragen Diagnostics Inc., Indianapolis, IN) of known, uniform size and refractive index. The value of Σ_t and the phase function $S(\theta)$ of this suspension can be predicted from Mie scattering theory,[33,34] assuming that the concentration of microspheres is low enough that they behave as independent scattering particles. The microspheres used were either 2.26 ± 0.018 or $0.173 \pm 0.007\,\mu$m in diameter, with a refractive index of 1.59 at 589 nm (manufacturer's data). This refractive index was assumed correct for 632.8 nm. The suspensions were made afresh for each use, to avoid changes in the optical properties due to aggregation. It was also observed that the properties changed over about one year, so that only new stock solutions were used.

These microspheres are close to being purely scattering with negligible light absorption. To test the technique for measuring Σ_t at the other extreme, namely a pure absorbing medium, India ink was used at a range of dilutions in water. These solutions were also measured in a standard spectrophotometer at 630 nm.

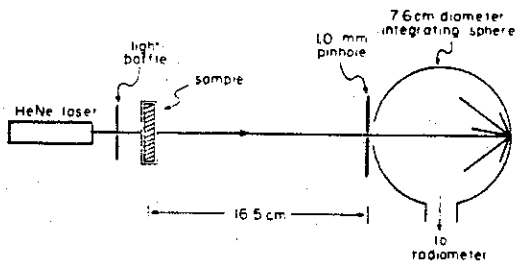

FIG. 1. Experimental arrangement for measuring the total attenuation coefficient, Σ_t (not to scale).

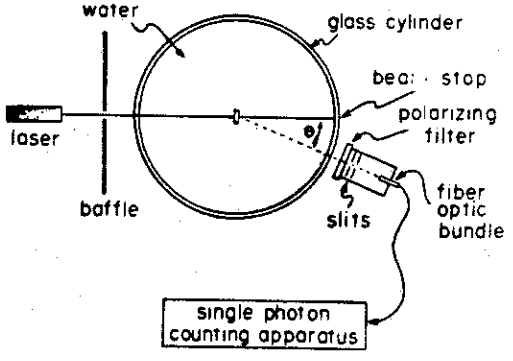

FIG. 2. Experimental arrangement for measuring the scattering phase function, $S(\theta)$ (not to scale).

B. Scattering phase function

The apparatus used to measure the scattering phase function $S(\theta)$, is illustrated in Fig. 2. The sample, prepared as above, was placed at the center of a 30-cm-diam cylindrical tank of distilled water, and irradiated by the laser beam. A light baffle was placed between the laser and the tank to reduce the background light from the laser tube. The water tank reduced both specular reflection at the cuvette or cover slip faces, and the refraction of scattered photons. The water was prefiltered (2-μm Whatman filter) to minimize light scattering from, e.g., dust particles. The detector arm, which was manually rotated about the sample in the plane of the laser beam, held an optical fiber bundle and slit assembly with an angular resolution of $\pm 0.1°$. The total uncertainty in the scattering angle θ, including the error in positioning of the detector arm, was $\simeq \pm 0.3°$. The smallest angle at which measurements were made was 2.4° in order to avoid the transmitted unscattered beam. Generally, the sample was kept fixed at 90° to the laser beam, so that $S(\theta)$ was not determined for scattering angles between 70° and 110° due to the edges of the sample holder. The sample could be rotated to fill this gap, and this was done in the case of the microspheres, where the 90° scattering was of particular interest. Slit collimation was used in front of the fiber bundle to further reduce light background, and a linear polarizing filter could also be inserted in this position. The sample thicknesses used were as small as possible to minimize multiple scattering effects ($<100\,\mu$m for tissues, 1 mm for phantom media). For each sample and scattering angle, the signal obtained using distilled water in the sample cell was subtracted from that with tissue in order to correct for light scattered by the sample cell and the water tank. The background was significant compared to the sample signal only for the dilute liquid media. $S(\theta)$ was then calculated by dividing the resulting values by the integral of the values over solid angle, with linear interpolation for missing data points. For tissues, each experiment was repeated three times on separately prepared samples from the same batch.

As in the case of Σ_t, in order to check this experimental technique, $S(\theta)$ was measured for the polystyrene microspheres, and the results compared with Mie theory. Both as predicted by theory and retrospectively from the measurements of Σ_t, the mean free path for the microsphere concentrations used, namely 0.0058% and 0.022% solids for the large and small spheres, respectively, was ~10 mm. This is an order of magnitude greater than the sample thickness, so that multiple scattering should only minimally distort the measured phase functions. The microsphere experiments were carried out with a linear polarizing filter in the detector arm, for polarization either parallel or perpendicular to the scattering plane. This permits a more rigorous test against Mie theory than with unpolarized light. The incident laser beam was not polarized for any of the experiments.

III. RESULTS

A. Total attenuation coefficients

Figure 3 shows the total attenuation coefficient of the 2.26-μm-diam microspheres, compared with the corresponding Mie theory prediction. The best fit to the data gives a measured value of $\Sigma_t (\sim \Sigma_s) = 0.172 \pm 0.005\ \text{mm}^{-1}$ for 0.01% concentration of solids. This is in excellent agreement with the Mie prediction of $0.175 \pm 0.002\ \text{mm}^{-1}$, based on the particle size and refractive index. The transmitted light intensity through the sample cell as a function of microsphere concentration was found to obey Beer's Law up to a concentration of ~0.4% solids, indicating that the microspheres acted as independent scattering centers.[33]

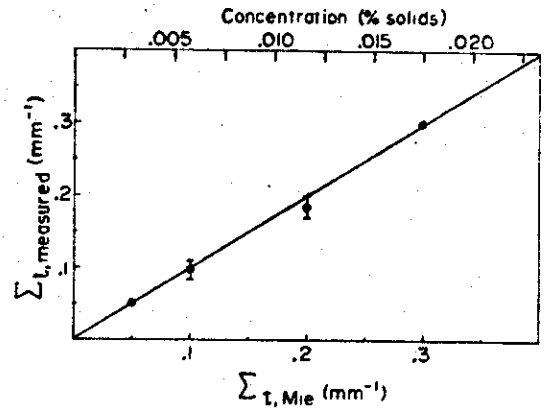

FIG. 3. Comparison of the measured values of Σ_t and the Mie theory predictions, for increasing concentration of 2.26-μm microspheres. For two points, the error bars are smaller than the symbol size.

In the case of India ink used as a pure absorbing medium, the measured value for a standard concentration was $\Sigma_t (\sim \Sigma_a) = 4.21 \pm 0.16\ \text{mm}^{-1}$, in reasonably good agreement with the value of $4.63 \pm 0.07\ \text{mm}^{-1}$ obtained spectrophotometrically.

The total attenuation results for the five tissues measured are shown in Figs. 4(a)–4(e), as a function of the thickness of the tissue sample. Each point in these plots corresponds to a single light transmission measurement. A new sample was prepared for each measurement, but all samples for a given tissue were taken from the same gross piece of tissue. The straight lines in these plots are the least-squares fits to the data, and the values of Σ_t, summarized in Table I, were calculated from these assuming Eq. (4).

As a check that our Σ_t values were not distorted due to multiple scattering in the tissue samples, we show in Fig. 4(f) the attenuation plot for chicken muscle, including measurements for sample thicknesses of 500 and 1000 μm. It is apparent that multiply scattered photons are detected, but that this does not seriously affect the measurements in samples less than about 100 μm thick. Any small residual multiple scattering would cause Σ_t to be underestimated in these experiments.

We have not presented the plots for blood and Nutralipid since they show negligible deviation from a straight line through the origin. The sample-to-sample variation was also very small. We have not investigated the subject-to-subject variation for blood, nor attempted to quantitate any systematic errors in the measurements for blood or Nutralipid. The measured values for the attenuation coefficients are given in Table I.

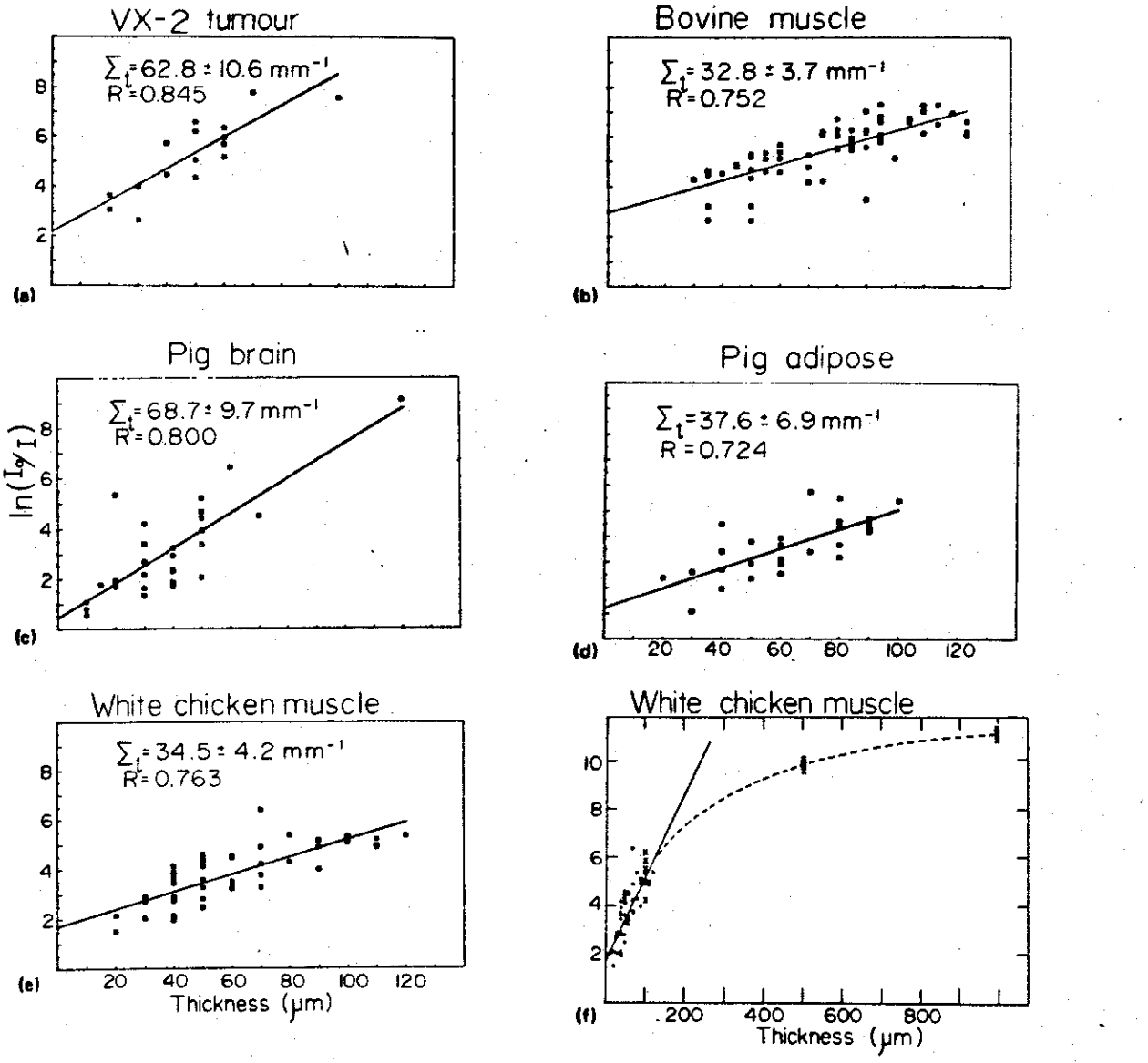

FIG. 4. Narrow-beam attenuation data for the five tissues, for increasing thickness of the tissue sample. Each point represents a separate measurement on a different tissue sample. The straight lines in (a)–(e) are the least-squares fits for Σ_t with regression coefficients R. (f) The measurements represented by ● and the straight-line fit are as for (e) with the tissue held between glass cover slips. For the thicker samples (×) cuvettes were used. The arbitrary dashed line shows the deviation from linearity resulting from detection of multiple scattered photons.

TABLE I. Experimental values of the total attenuation coefficient and the average cosine of scattering.

Tissue/medium	This work	Σ_t (mm^{-1}) from Ref. 11 using $\Sigma_t = \Sigma_a + \Sigma_s'/(1-\bar{\mu})$	Other published values	This work	$\bar{\mu}$ Other published values
Chicken muscle	34.5 ± 4.2	23 ± 3[a]	0.43[b]	0.965 ± 0.004	0.0[b]
Bovine muscle	32.8 ± 3.7	15 ± 8[a]	0.83[b]	0.954 ± 0.016	0.3[b]
Pig brain	68.7 ± 9.7	95 ± 46[a]		0.940 ± 0.029	
Pig adipose	37.6 ± 6.9			0.771 ± 0.063	
VX2 tumor rabbit ear	62.8 ± 10.6			0.639 ± 0.067	
Human blood (1%)	2.9		2.0[c], 1.4[d]	0.974	>0.99[e]
Nutralipid (1%)	3.84	4.8		0.690	

[a] Errors calculated from errors in $\bar{\mu}$.
[b] Reference 6.
[c] Reference 36.
[d] Reference 37.
[e] Reference 39.

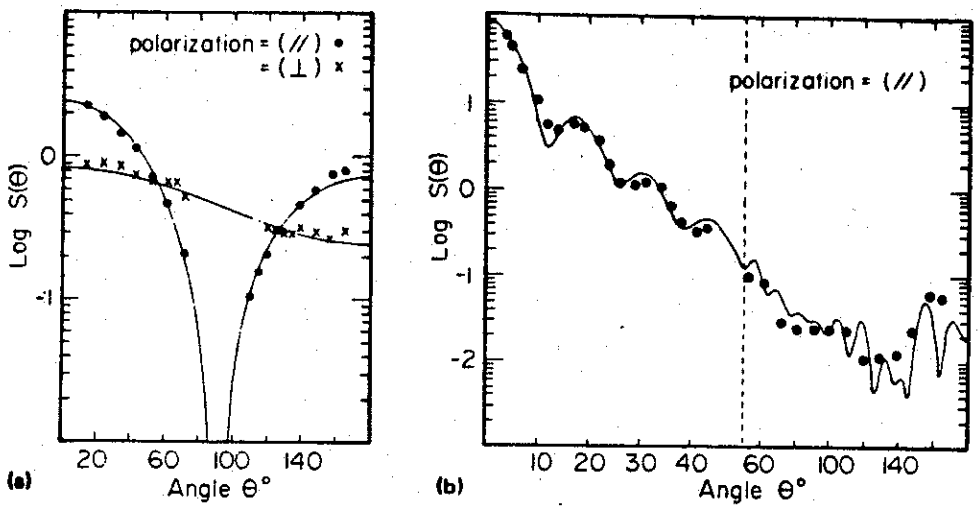

FIG. 5. Scattering phase functions for (a) 0.173-μm microspheres and two different light polarizations and (b) 2.26-μm microspheres and parallel light polarization. Note the change in the θ scale at 50°. The curves are the corresponding Mie theory predictions. The experimental and theoretical values are independently normalized (see text).

B. Scattering phase functions

Considering first the microsphere results, Fig. 5(a) shows the experimental values for $S(\theta)$ versus θ for the smaller, 0.173-μm-diam microspheres, for parallel and perpendicular polarizations, together with the Mie theory predictions. This is a very sensitive test of the experimental method, and, as can be seen, the shape of the phase functions is in excellent agreement with Mie theory. Figure 5(b) shows, on an expanded scale, a more detailed plot of the scattering phase function for the larger microspheres, for parallel polarization. It can be seen that the data tend to follow the fine structure of the Mie function, especially in the forward direction where the scattered light signal is strongest compared with the background. The perpendicular polarization data (not shown) also agree with Mie theory as they did for the smaller microspheres.

The phase function results for the tissues are shown in Figs. 6(a)–6(e). For each tissue, two to three sets of measurements were made on separate samples. Each set of raw data was then normalized to unit integral for these plots. For blood and Nutralipid, shown in Fig. 6(f), there was negligible sample-to-sample variation.

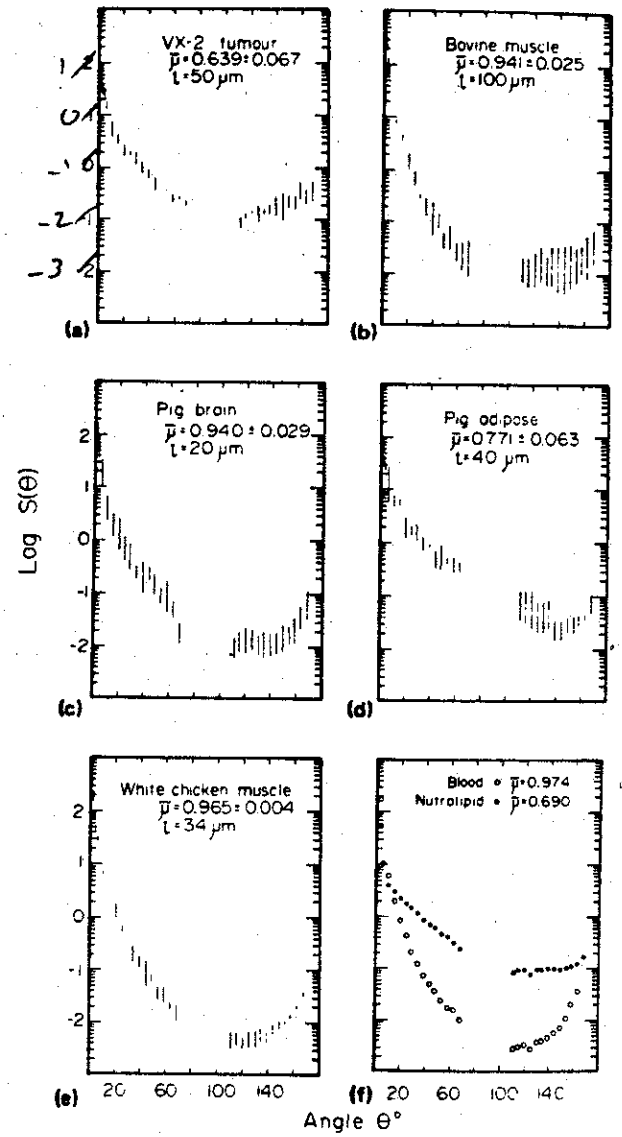

FIG. 6. (a)–(e) Scattering phase functions for the five tissues (sample thickness t). The vertical bars give the range of values found between the self-normalized data from several different tissue samples. The errors in $\bar{\mu}$ are calculated from the sample-to-sample variance. (f) Scattering phase functions for 1% blood and 0.1% Nutralipid solution (single measurements).

IV. DISCUSSION

A. Total attenuation coefficients

The results for Σ_t in polystyrene microspheres (Fig. 3) provide strong confirmation of the validity of the narrow-beam method. For each of the tissues shown in Fig. 4 there is a large scatter in the data. This could be due to real variations in Σ_t from sample-to-sample, and certainly considerable animal-to-animal variability in tissue properties such as Σ_{eff} has been observed in most other studies, both *in vivo* and *in vitro*.[1] Alternatively, or in addition, the scatter could be due to tissue handling and preparation, as discussed below. The fact that the fitted lines in Fig. 4 do not pass through the origin is believed to be an artifact due to imperfect surface contact between the tissues and the glass sample cells, causing additional light loss from surface scattering compared with the water-filled cell. The attenuation plots do go

through the origin for the liquid Nutralipid and blood samples, as expected. This effect should not alter the values of Σ_t for tissues, which are derived from the slope of the attenuation curves.

There are a number of comparisons possible between our measured Σ_t values and other data. First, we may combine the values for $\bar{\mu}$ shown in Fig. 6 with measurements of Σ_a and $\Sigma_s'[=(1-\bar{\mu})\Sigma_s]$ recently obtained in this laboratory[11] using an indirect "added absorber" technique. Taking $\Sigma_t = \Sigma_a + \Sigma_s'/(1-\bar{\mu})$ then gives values for chicken and bovine muscle of ~23 and 15 mm^{-1}, respectively, i.e., of the same order as the direct measurements above. Likewise, for pig brain the direct and indirect values are 68.7 and 95 mm^{-1}. Using indirect techniques *in vitro* at 633 nm, Wilksch *et al.*[7] and recently Cheong *et al.*[23] have reported Σ_t values of 4.1 and 8.9 mm^{-1} for pig muscle and human bladder tissue, respectively. At other wavelengths, Crilly[35] measured $\Sigma_t \sim 7$–40 mm^{-1} for human breast tissues between 700 and 1200 nm, while Jacques and Prahl[24] obtained values of 24.1 mm^{-1} for mouse dermis at 488 nm. These data all indicate that the Σ_t values of lightly pigmented soft tissues are typically in the range 10^1–10^2 mm^{-1} in this spectral region. However, substantially lower values (0.43 and 0.83 mm^{-1} for chicken and bovine muscle, respectively) were found by Marynissen and Star[6] using an interstitially placed, collimated optical fiber coupled to a photodetector to measure the decrease in primary light flux with depth in intact tissue. A possible explanation, given the very forward nature of scattering as found in the present study and as recently reported by others,[23,24,35] is that the detector fiber used was not sufficiently collimated to reject all the forward scattered light.

For blood, our value of $\Sigma_t = 2.9$ mm^{-1} for a 100:1 dilution of human whole blood may be compared with the value of 2.0 mm^{-1} of Zdrojkowski and Longini[36] and 1.4 mm^{-1} of Pedersen *et al.*[37] These results are in reasonable agreement, considering that the measurement techniques were very different and that the physiological conditions were not strictly comparable in the three studies. It is of interest to estimate the contribution of absorption to Σ_t in the case of blood. Assuming that all absorption at 632.8 nm is due to hemoglobin, Σ_a for 1% concentration of blood is ~0.1 and 0.01 mm^{-1} for hemoglobin and oxyhemoglobin, respectively.[10,38] Thus, blood is highly scattering, with an albedo > 0.96 when deoxygenated and > 0.99 when fully oxygenated (for $\Sigma_t = 2.9$ mm^{-1}). For Nutralipid, our value of 3.84 mm^{-1} for 1% concentration of solids is in reasonable agreement with 4.8 mm^{-1} predicted from the added absorber measurements.[11]

B. Scattering phase functions

As was the case with Σ_t, the excellent agreement between the measurements and Mie theory for the polystyrene microspheres lends credibility to the tissue results. It is of interest to note in Fig. 6 the good reproducibility in the tissue measurements of $S(\theta)$, evidenced by the relatively small range of values found between samples. The highly forward nature of the scattering in tissue is confirmed by other indirect studies in human epidermis,[30] mouse dermis,[24] pig muscle,[7] and human bladder wall.[23] It disagrees with the nearly isotropic scattering found by Marynissen and co-workers[6,9] in chicken and bovine muscle ($\bar{\mu} = 0, 0.3$, respectively) obtained by comparing the radiance pattern measured at depth in tissue with the numerical results of van de Hulst.[27] However, this required the use of Σ_t data to yield a unique solution for Σ_a, Σ_s, and $\bar{\mu}$, and, as noted above, the Σ_t values found in these experiments are much lower than in most recent studies. Therefore it is possible that these radiance measurements would be consistent also with highly forward scattering and Σ_t values in the 10^1–10^2 mm^{-1} range.

The scattering phase functions found for soft tissues, if interpreted according to Mie theory, lead to scattering particle sizes in the micron diameter range, i.e., comparable to small cells or major internal structures of large cells ($\bar{\mu} > 0.8$ for particle diameter > 0.5 μm and refractive index = 1.4). The fact that the one tumor measured was not so strongly forward peaked as the normal tissues may be connected with the altered microstructure of malignant tissue, or may result from, for example, necrotic debris which is submicron is size and hence more isotropically scattering. More systematic studies are required to determine the light scattering structures within normal and malignant tissues.

For blood, our measured value of $\bar{\mu} = 0.974$ is comparable with that found by Reynolds[39] by an indirect reflectance technique, namely $\bar{\mu} > 0.99$. The low value for Nutralipid ($\bar{\mu} = 0.690$) might suggest that this is not a good phantom material to simulate the optical properties of tissues, since the particle size is too small (99% < 1 μm: private communication, Pharmacia, Inc.). However, use of the similarity principle described by van de Hulst[27] may make it possible to adjust the Nutralipid concentration (controlling Σ_s) and the amount of added absorber (Σ_a) to compensate for this.

C. Effects of tissue preparation

In the experiments reported here involving the use of very thin tissue samples, the tissues were subjected to grinding and/or freezing. Thus, there is the possibility that these procedures, and indeed the use of *postmortem* specimens, changes the optical properties of the tissues from their *in vivo* values. This has not been systematically examined, and clearly this needs to be done for cases where the *in vivo* optical properties must be determined accurately. For example, we have shown in a previous study[10] that Σ_{eff} may change by a factor of 2 or more in the visible wavelength range within 1-h *postmortem*, even *in situ*. It is known also that freezing and thawing may alter the transmission of light through thick tissue samples.[40] However, there is reason to believe that the conclusions of the present work regarding Σ_t and $S(\theta)$ will not be substantially different from the true situation *in vivo*. In the first instance, there was agreement to within a factor of 2 between the values of Σ_t found in the direct measurements here, and the indirect added absorber experiments of Wilson *et al.*,[11] where the tissues were not frozen and were only very coarsely ground. Second, we have measured Σ_t directly for one sample of chicken muscle which was freshly cut without grinding or freezing, and obtained a value which was two-thirds of the mean for the ground, frozen tissue. Third, in other recent reports[23,24,35] of high attenuation and

high forward scattering, tissues were intact and had not, to our knowledge, been frozen. Finally, for $\bar{\mu}$ it is likely that effects such as cell lysis, which could result from freezing and grinding, would tend to decrease rather than increase the average scattering particle size, and hence cause $\bar{\mu}$ to be underestimated.

V. CONCLUSIONS

The values for Σ_t and $S(\theta)$ of the various tissues measured here are not presented as a systematic or comprehensive set of data. Rather, the purpose of the study was to define order of magnitude of these parameters for typical tissues. The main value of these data lies not in the actual detailed values found for these tissues, but in the guidance they provide in developing appropriate experimental techniques for more systematic and extensive measurements of the optical properties of tissues, and in developing relevant models of light propagation.

The main conclusions from the results presented above are that, for 630 nm of light in lightly pigmented soft tissues:

(1) the mean free path is very small, typically $\sim$10–100 μm ($\Sigma_t \sim 10^1$–10^2 mm^{-1}); and

(2) the scattering is very forward peaked, with $\bar{\mu}$ greater than 0.95 in some normal tissues, and >0.6 for all tissues measured.

In addition, other indirect measurements[11,23,24] of the relative contributions of absorption and scatter indicate that light propagation is scatter dominated, with Σ_s/Σ_a being typically $\sim 10^2$–10^3. These findings define the conditions under which future experimental and theoretical studies of light dosimetry for PDT must be developed. Finally, we note that the high forward scattering means that there is a large difference between the scattering coefficient Σ_s, which describes the fundamental scattering interactions, and the "reduced" scattering coefficient Σ_s' which describes the effective scattering conditions within the diffusion region. Also, a small change in $\bar{\mu}$ produces a large change in Σ_s'; for example a change from 0.96 to 0.97 decreases Σ_s' by 25%. Thus knowledge of the phase function, or $\bar{\mu}$, is important for modeling light propagation in tissue, not only near the irradiated surface but also at depth. Similarly, in tissues with high albedo the space irradiance distribution is very sensitive to the absorption coefficient, so that it is essential to develop methods to determine Σ_a accurately. As mentioned in the Introduction, the high albedo of tissue makes this very difficult to do by direct methods, although a possible technique has been proposed,[32] which is currently being investigated in this laboratory.

ACKNOWLEDGMENT

This work was supported by the National Cancer Institute of Canada.

[a] Address correspondence to: Brian C. Wilson, Departments of Physics, Hamilton Regional Cancer Centre and McMaster University, 711 Concession Street, Hamilton, Ontario, Canada L8V 1C3.

[1] B. C. Wilson and M. S. Patterson, Phys. Med. Biol. 31, 327 (1986).
[2] J. J. Duderstadt and L. J. Hamilton, *Nuclear Reactor Analysis* (Wiley, New York, 1976), p. 103.
[3] D. R. Doiron, L. O. Svaasand, and A. E. Profio, in *Porphyrin Photosensitization*, edited by D. Kessel and T. J. Dougherty (Plenum, New York, 1983), p. 63.
[4] L. E. Preuss, F. P. Bolin, and B. W. Cain, Photochem. Photobiol. 37, 113 (1983).
[5] D. R. Doiron, in *Porphyrin Localization and Treatment of Tumors*, edited by D. R. Doiron and C. J. Gomer (Liss, New York, 1984), p. 41.
[6] J. P. A. Marynissen and W. M. Star, in Ref. 5, p. 133.
[7] P. A. Wiksch, F. Jacka, and A. J. Blake, in Ref. 5, p. 149.
[8] B. C. Wilson, W. P. Jeeves, D. M. Lowe, and G. Adam, in Ref. 5, p. 115.
[9] J. P. A. Marynissen, W. M. Star, J. L. van Delft, and N. A. P. Franken, in *Photodynamic Therapy of Tumors and Other Diseases*, edited by G. Jori and C. Perria (Libreria Progetto Editore, Padova, 1985), p. 387.
[10] B. C. Wilson, W. P. Jeeves, and D. M. Lowe, Photochem. Photobiol. 38, 153 (1985).
[11] B. C. Wilson, M. S. Patterson, and D. M. Burns, Lasers Med. Sci. 1, 235 (1986).
[12] J. Eichler, J. Knof, and H. Lenz, Rad. Environ. Biophys. 14, 239 (1977).
[13] A. E. Profio and D. R. Doiron, Med. Phys. 8, 190 (1981).
[14] M. J. C. van Gemert and J. P. Hulsenbergen Henning, Arch. Dermatol. Res. 270, 429 (1981).
[15] S. Wan, R. R. Anderson, and J. A. Parrish, Photochem. Photobiol. 34, 493 (1981).
[16] R. R. Anderson, J. Hu, and J. A. Parrish, in *Bioengineering and the Skin*, edited by R. Marks and P. A. Payne (MTP Press, Lancaster, PA, 1981), p. 253.
[17] L. O. Svaasand and R. Ellingsen, Photochem. Photobiol. 38, 283 (1983).
[18] M. J. C. van Gemert, M. C. Berenbaum, and G. H. M. Gijsberg, Br. J. Cancer 52, 43 (1985).
[19] L. O. Svaasand and R. Ellingsen, Photochem. Photobiol. 41, 73 (1985).
[20] M. J. C. van Gemert, A. J. Welch, J. J. M. Bonnier, J. W. Valvano, G. Yoon, and S. Rastegas, Sem. Int. Radiol. 3, 27 (1986).
[21] B. C. Wilson, P. J. Muller, and J. C. Yanch, Phys. Med. Biol. 31, 125 (1986).
[22] P. J. Muller and B. C. Wilson, Phys. Med. Biol. 31, 1295 (1986).
[23] W. F. Cheong, M. Motamedi, and A. J. Welch, Lasers Surg. Med. 7, 72 (1987).
[24] S. L. Jacques and S. A. Prahl, Lasers Surg. Med. 6, 494 (1986).
[25] V. P. Kubelka and F. Munk, Z. Tech. Phys. 12, 593 (1931).
[26] V. P. Kubelka, J. Opt. Soc. Am. 38, 448 (1948).
[27] H. C. van de Hulst, *Multiple Light Scattering Tables, Formulas and Applications* (Academic, New York, 1980).
[28] B. C. Wilson and G. Adam, Med. Phys. 10, 824 (1983).
[29] A. L. McKenzie, Phys. Med. Biol. 30, 455 (1985).
[30] W. A. G. Bruls and J. C. van der Leun, Photochem. Photobiol. 40, 231 (1984).
[31] R. Baghdassarian, M. W. Wright, S. A. Vaughn, M. W. Berns, D. C. Martin, and A. G. Wile, J. Urol. 133, 126 (1985).
[32] B. C. Wilson, M. S. Patterson, and S. T. Flock, Photochem. Photobiol. (in press).
[33] H. C. van de Hulst, *Light Scattering by Small Particles* (Dover, New York, 1957).
[34] C. F. Bohren and D. R. Huffman, *Absorption and Scattering of Light by Small Particles* (Wiley, New York, 1983).
[35] R. Crilly, Med. Phys. 13, 603 (1986) (Abstract).
[36] R. J. Zdrojkowski and R. L. Longini, J. Opt. Soc. Am. 59, 898 (1969).
[37] G. D. Pedersen, N. J. McCormick, and L. O. Reynolds, Biophys. J. 16, 199 (1976).
[38] O. W. van Assendelft, *Spectrophotometry of Hemoglobin Derivatives* (Royal Vangorcum, Netherlands, 1970).
[39] L. O. Reynolds, Ph.D. thesis, University of Washington, 1975.
[40] L. E. Preuss, F. P. Bolin, and R. C. Taylor, Photochem. Photobiol. S43, 32 (1986) (Abstract).